JACS
JOURNAL OF THE AMERICAN CHEMICAL SOCIETY

Article

pubs.acs.org/JACS

Structural Role of Counterions Adsorbed on Self-Assembled Peptide Nanotubes

Frédéric Gobeaux,*[,†,§] Nicolas Fay,[†,§] Christophe Tarabout,[§] Cristelle Mériadec,[§] Florian Meneau,[∥] Melinda Ligeti,[‡] David-Alexandre Buisson,[‡] Jean-Christophe Cintrat,[‡] Khac Minh Huy Nguyen,[†] Lionel Perrin,[⊥] Céline Valéry,[#,¶] Franck Artzner,[§] and Maïté Paternostre*[,†]

[†]Institut de Biologie et de Technologies de Saclay/Service de Bioénergétique and [‡]Institut de Biologie et de Technologies de Saclay/Service de Chimie Bioorganique et Marquage, Biologie Structurale et Mécanismes, Commissariat à l'Énergie Atomique et aux Énergies Alternatives-Saclay, 91191 Gif-sur-Yvette, France

[§]Unité Mixte de Recherche 6251, Centre National de la Recherche Scientifique and Université Rennes 1, 35042 Rennes, France

[∥]SWING Beamline, SOLEIL Synchrotron, 91191 Gif-sur-Yvette, France

[⊥]Laboratoire de Physique et Chimie de Nano-Objets, CNRS INSA, 31077 Toulouse Cedex 4, France

[#]Ipsen Pharma S.A., Ctra. Laurea Miro 395, 08980-Sant Feliu de Llobregat, Barcelona, Spain

Supporting Information

ABSTRACT: Among noncovalent forces, electrostatic ones are the strongest and possess a rather long-range action. For these reasons, charges and counterions play a prominent role in self-assembly processes in water and therefore in many biological systems. However, the complexity of the biological media often hinders a detailed understanding of all the electrostatic-related events. In this context, we have studied the role of charges and counterions in the self-assembly of lanreotide, a cationic octapeptide. This peptide spontaneously forms monodisperse nanotubes (NTs) above a critical concentration when solubilized in pure water. Free from any screening buffer, we assessed the interactions between the different peptide oligomers and counterions in solutions, above and below the critical assembly concentration. Our results provide explanations for the selection of a dimeric building block instead of a monomeric one. Indeed, the apparent charge of the dimers is lower than that of the monomers because of strong chemisorption. This phenomenon has two consequences: (i) the dimer−dimer interaction is less repulsive than the monomer−monomer one and (ii) the lowered charge of the dimeric building block weakens the electrostatic repulsion from the positively charged NT walls. Moreover, additional counterion condensation (physisorption) occurs on the NT wall. We furthermore show that the counterions interacting with the NTs play a structural role as they tune the NTs diameter. We demonstrate by a simple model that counterions adsorption sites located on the inner face of the NT walls are responsible for this size control.

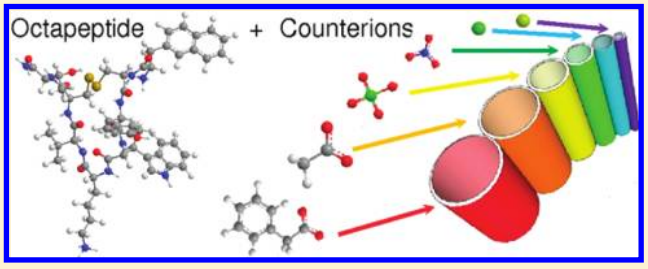

INTRODUCTION

Charges and counterions are known to play a crucial role in a vast number of physical, chemical, and biological systems. Indeed, electrostatic interactions between charged objects in solutions are controlling not only the colloidal stability but also the folding and biological activity of proteins,[1] the compaction of the genetic material,[2] the adsorption of ions onto lipid membranes,[3] and the self-assembly of biomolecules, such as actin and microtubules.[4] In some cases, these effects are purely due to electrostatic effects, i.e., to the number of charges in solution set by background salts. In other cases, the salt effect is also specific and depends on the nature of the ion. These specific effects are ubiquitous and have been categorized as "Hofmeister effects".[5,6]

The literature dealing with the direct effect of counterions on macromolecular assemblies is rather scarce. Such studies are mainly restricted to the field of surfactant micellization, such as alkylammonium salts.[7−10] These works establish a correlation between the propensity of the counterions to form ion pairs with the surfactant headgroups and the critical micellization concentration. Another example of structural effect of counterions has been observed in catanionic mixtures of surfactants where the progressive exchange of HO^- by other anions promotes the stability of a new lamellar phase.[11] Also, many papers from R. Oda's group highlight the structural role of counterions with Gemini surfactants.[12] Chiral counterions, such as tartrate, malate, or gluconate, were shown to induce new morphologies, such as twisted ribbons, in nonchiral surfactants.[13] Notably, the chiral counterions were accurately localized in the structure, and their packing has been related to the expression of the chirality at a mesoscopic scale.[14] Even

Received: November 2, 2011
Published: December 2, 2011

   dx.doi.org/10.1021/ja210299g | J. Am. Chem.Soc. 2012, 134, 723−733

more complex anions, such as peptides[15] or nucleotides,[16] have been introduced to form hydrogelling aggregates. Another example worth mentioning is the case of metal ions coordination bondings whose direct role in the assembly and rheology of peptide amphiphile nanofibers has been observed by Stendahl et al.[17] Finally, the concept of "structural counterions" has been proposed by F. Grohn to describe how the stacking of aromatic counterions can promote the assembly of dendrimeric molecules.[18,19]

The question behind these studies is can we trigger self-assemblies or control their size and morphology with the help of counterions? To achieve this, the counterions in the molecular structure need to be localized so as to identify relevant lever arms.[14] The scarcity of studies is also due to a lack of experimental model systems that allow observing changes in supramolecular assembly without simply destroying it.

Lanreotide is a dicationic octapeptide, usually used as an acetate salt, that exhibits remarkable self-assembly properties in pure water. Above a critical assembly concentration (CAC) of 20 mM, the peptide spontaneously self-assembles into monodisperse, hollow nanotubes (NTs) of 24.4 nm diameter. These NTs, separated from each other by a constant 12 nm distance, form a hexagonal columnar phase that coexists with the liquid phase up to 100 mM (ref 20 and Figure 1a). Moreover, it has been determined that the NT walls are formed by a 2D crystalline bilayer. The packing of the peptide in these two layers is different,[21] but both are structured in one direction by a H-bound network forming an antiparallel β-sheet and in the other by close contacts between lateral chains either in the β-turn or at the N-ter of the molecule (see Figure 1a). These close-contacts are particularly important in that they tune the NTs diameter.[22] Finally, the recently elucidated mechanism of lanreotide NT formation shows that the molecule undergoes a monomer-to-dimer equilibrium characterized by a dissociation constant K_d of about 5 mM and that in the early stages of assembly open ribbons coexist with short NTs, suggesting a transition state corresponding to the closure of open ribbons into NTs. We have proposed that this final step could be regulated by a subtle balance between attractive forces and electrostatic repulsions.[23]

Many observations suggest that electrostatics plays a prominent part in that self-assembly process, although it has not been studied in detail so far: (i) despite a high content in aromatic residues, the peptide is highly soluble as indicated by the high CAC;[23] (ii) the hexagonal parameter of the columnar phase is insensitive to concentration, suggesting that electrostatic forces are stabilizing the hexagonal phase;[20,21] this parameter, equal to 36 nm, corresponds to a rather long-range interaction;[24] and (iii) the mechanism of NT formation suggests that the monodispersity of the system is due to a fine balance between forces of opposite signs. Moreover, among other observations, it is still not understood why the building block of the NTs is not the monomer but the dimer that possesses twice as many charges and should thus be more repulsive.

In this work, we focus on the interactions between all the charged species coexisting in the solution and on the possible structural role of the counterions. A combination of experimental approaches that includes osmometry, transmission electron microscopy (TEM), small-angle X-ray scattering (SAXS), and Fourier-transform infrared spectroscopy (FTIR) has been used to assess the role of the peptide cationic charges and their counterions in lanreotide self-assembly. In particular, comparative studies were carried out with different types of counterions and charge-modified peptides deriving from lanreotide. Through these experiments we have found out that most counterions are adsorbed on very specific sites and evidenced their structural role resulting from their location.

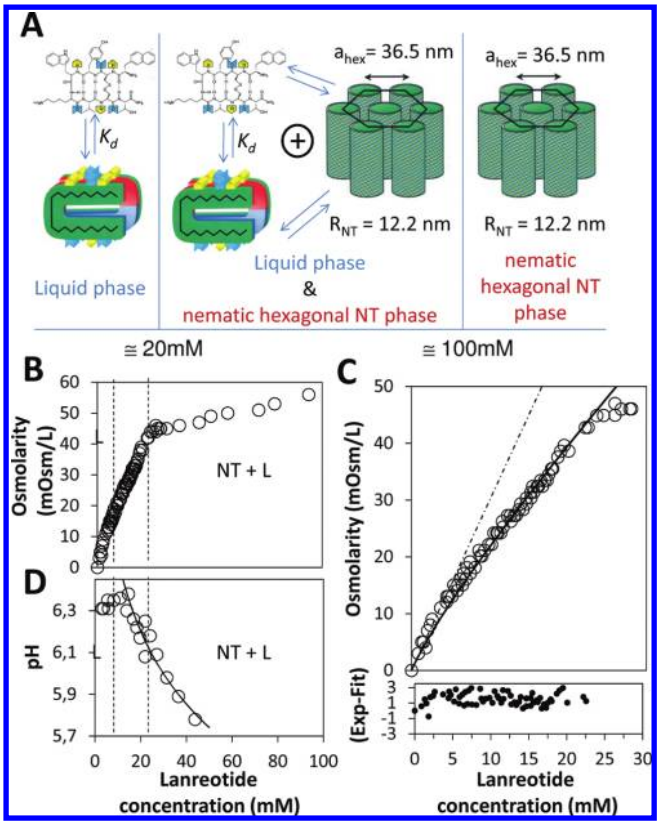

Figure 1. Sequence of phases, osmolarity, and pH measurements. (a) Sketches describing the different self-assembly states of the lanreotide salt as a function of concentration. Up to 20 mM, the peptide undergoes a monomer-to-dimer equilibrium (L domain). Between 20 and 100 mM, coexistence of the liquid phase and a hexagonal nematic NT phase (NT+L domain). Above 100 mM, a pure hexagonal nematic NT phase (NT domain). (b) Evolution of the osmolarity of lanreotide-acetate solutions with concentration and boundary between the L and NT+L domains (see text for details). (c) Zoom on the L domain. The dashed straight lines are the lines fitting the data at low and high concentration of domain L and have a slope of 3 and 1.7 (low and high concentrations, respectively). The plain line is a fit taking into account the monomer−dimer equilibrium and the dissociation of the counterions from the peptides (see text for details). (d) Evolution of the pH in the domains L and NT+L. The decreasing part of the plot is fitted using a logarithmic law pH = $-1.16*\log(C_{lanreotide}) + 7.7$.

RESULTS

The concentration−temperature phase diagram of the lanreotide-acetate salt in pure water was established a few years ago.[20] In the present study, we focus on the low-concentration part of the phase diagram, i.e., below 100 mM. From previous studies, we know that the peptide salt in solution undergoes a monomer-to-dimer equilibrium and that above 20 mM the dimers self-assemble into very long (a few hundreds of micrometers) NTs with a monodisperse diameter of 24.4 nm. These NTs form a hexagonal phase coexisting with the liquid phase containing the monomers and dimers (Figure 1a). The following results are divided into two parts. The first one

dx.doi.org/10.1021/ja210299g | J. Am. Chem.Soc. 2012, 134, 723−733

focuses on the characterization of the liquid phase only, either below or above the CAC. In the second part, the effects of counterion exchange and charge suppression on the structure and morphology of the NTs are addressed.

Physicochemical Characterization of the Lanreotide Liquid Phase Either Alone or in Equilibrium with the NTs. To characterize the dissociation state of the peptide salt either below or above the CAC, we have measured the osmolarity of solutions in a concentration range covering the liquid phase and the liquid−NT coexistence domain,[20] i.e., up to 100 mM (Figure 1b). From now on, these two domains will be referred to as the "L domain" and the "NT+L domain", respectively. Osmolarity is a measure of the concentration of solute particles in a solution, regardless of their nature. In the case of charged species, it gives information on the dissociation state of the molecule and its counterions. For example, 1 mM of monomer of a fully dissociated lanreotide-acetate salt should lead to 3 mOsm/L (one monomer + two acetates) and 1 mM of dimer to 5 mOsm/L (one dimer + four acetates). The plot of osmolarity as a function of lanreotide-acetate concentration clearly exhibits two different regimes: up to 20 mM, the osmolarity strongly increases with the concentration, while above 20 mM, this increase is much slower. The rupture in the osmolarity increase corresponds well with the CAC previously determined. Indeed, the formation of lanreotide NTs results in an abrupt decrease of the evolution of osmolarity with peptide concentration, as the peptides forming the NTs are almost not contributing to the osmolarity.

The L Domain. Figure 1c zooms in the low-concentration part of the osmolarity plot, i.e., in the liquid phase below the CAC that we refer to as the "L domain". Up to 20 mM, the osmolarity of the solution continuously increases albeit not linearly. Indeed, whereas at low concentration the slope is close to 3 mOsm·L^{-1}·mM^{-1}, a value consistent with a solution essentially containing fully dissociated monomers (one peptide + two acetates), at the end of the L domain, the slope is close to 1.7 mOsm·L^{-1}·mM^{-1}. A similar behavior is observed when the acetates are replaced by other counterions (see Table S1, Supporting Information and the Experimental Section for details on the counterion exchange procedure). Such a nonlinear evolution of the plot is expected since the peptide undergoes a monomer-to-dimer equilibrium.[23] This equilibrium should thus be taken into account to accurately fit the osmolarity data. Moreover, the slope of the osmolarity plot at the end of the L domain ranges from 1.4 to 1.8 mOsm·L^{-1}·mM^{-1}, when it should rather be close to 2.5 mOsm·L^{-1}·mM^{-1} (or 5 mOsm·L per mM of dimer) for a solution containing mostly dimers. This suggests that the dimers are not fully dissociated from their counterions. Therefore, this partial dissociation should also be taken into account to fit the osmolarity plot over the whole domain. Using the K_d and the monomer concentration $[M]$, the dimer concentration $[D]$ can be written as $[D] = [M]^2/K_d$. As a consequence, the total lanreotide concentration before the appearance of NTs can be written as

$$[\text{lanreotide}] = [M] + 2*[D] = [M] + 2*[M]^2/K_d \quad (1)$$

and the total osmolarity π as

$$\pi = \alpha*[M] + \beta*[D] \quad (2)$$

$$\pi = \alpha*\frac{-K_d + \sqrt{K_d^2 + 8*K_d[\text{lanreotide}]}}{4} + \beta*\frac{K_d + 4*[\text{lanreotide}] - \sqrt{K_d + 8*K_d[\text{lanreotide}]}}{8} \quad (2')$$

'where α and β are the dissociation parameters that are equal to 3 and 5 in the case of a fully dissociated system. Using eq 2', we fit the evolution of the osmolarity with the peptide concentration in the L domain, using the K_d, α, and β as adjustable parameters. The best fit is obtained with $\alpha = 3 \pm 0.02$, $\beta = 2.1 \pm 0.03$, and $K_d = 11.1 \pm 0.4$ mM, a value close to the one of 5 mM previously determined in ref 23 (Figure 1c). Interestingly, if the α value is consistent with a complete dissociation of the counterions from the monomers, the β value of 2.1 indicates that the dimer in solution represents only two free particles instead of the five expected (the dimer and its four counterions). Because of the electroneutrality principle, these two particles have to be a cation and an anion. The anion being an acetate means that the dimer is a single charged cationic species because about three out of the four counterions remain closely associated to it and neutralize its three other charges.

The NT+L Domain. The concentration domain ranging from 20 to 100 mM is the domain where the liquid phase and the NTs coexist, as it has been described previously.[20] In this domain, the osmolarity plot can be fitted by a straight line with a slope of 0.17 mOsm·L^{-1}·mM^{-1}. In such a coexistence domain, the osmolarity of the liquid phase is principally set by the composition at the CAC, i.e., about 45 mOsm/L, because the number of NTs is negligible against the number of monomers, dimers, and counterions. Additionally, when a molecule joins a structure with a high aggregation number (which is the case with the NTs here), it does not add up to the osmolarity. Therefore, the increase detected should come from the counterions released from the peptides involved in the NTs, and the slope is a direct measurement of the counterion condensation on the NTs. For a complete release of the counterions, we would measure a slope of 2 mOsm·L^{-1}·mM^{-1}; on the contrary, a complete condensation of the counterions would lead to a plateau. Thus, the measured slope of 0.17 mOsm·L^{-1}·mM^{-1} indicates that ∼90% of counterions are condensed, whereas ∼10% remain free in solution.

We have also measured the evolution of the pH with the peptide concentration covering the L and NT+L domains (Figure 1d). This evolution shows that if the pH of the solution in the L domain is constant as expected for salt solutions, it decreases logarithmically as soon as NTs are formed, indicating that acidic species are released in the solution. As we will discuss later in detail, this means that the solution is no longer buffered by the monomers and dimers but by the NTs themselves.

Altogether, the physicochemical characterization of the liquid phase, either alone (L domain) or in coexistence with the NTs (NT+L domain), shows that

(i) The dimers strongly interact with their counterions. Interestingly, this strong interaction could explain why the dimers are the building blocks of the NTs; indeed, this strong interaction screens the charges and thus favors the attraction between dimers over the one between monomers.

(ii) In the NT-L domain, the osmolarity of the solution linearly increases with a slope of 0.17 mOsm.L^{-1}.mM^{-1} indicating that only 10% of the acetate counterions are

dx.doi.org/10.1021/ja210299g | J. Am. Chem.Soc. 2012, 134, 723−733

released in the solution, the rest being condensed on the NT wall. Simultaneously, a decrease in pH is measured.

Effect of Counterions Exchange and Charge Deletion on the Structure and Morphology of the NTs. The structural role of counterions and charges in lanreotide salt self-assembly was assessed by checking the consequences of anionic counterions exchange and of cationic charge suppression on the NTs structural features.

Figure 2 shows the characterization of lanreotide samples, for which the acetate counterions have been exchanged for a dozen

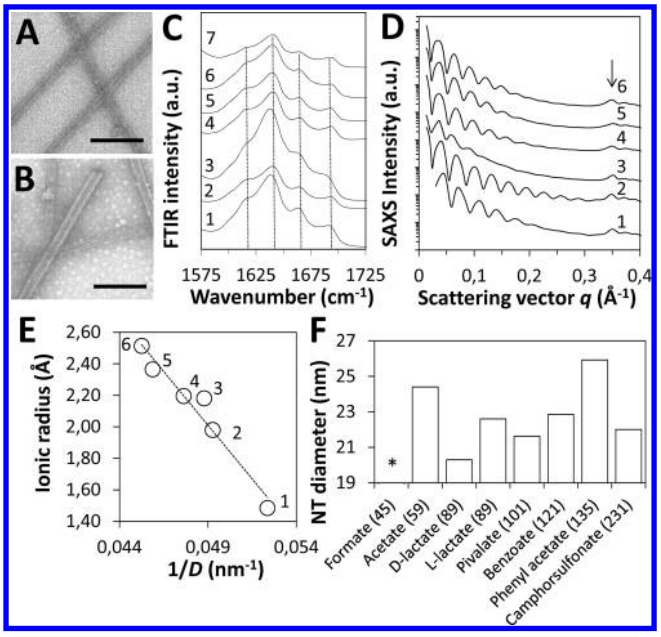

Figure 2. Counterions modulate NTs diameter. (a) TEM micrograph of negatively stained lanreotide NTs formed with fluoride or (b) benzoate as counterions. Scale bars: 200 μm. (c) Amide I region of the FTIR spectra of the peptide gels with different counterions (1, fluoride; 2, chloride; 3, bromide; 4, nitrate; 5, iodide; 6, perchlorate; and 7, acetate). (d) SAXS profiles for different counterions. (e) Plot of the spherical counterions ionic radii as a function of the inverse of the NT diameters. The arrow indicates the peaks due to the antiparallel β-sheets. (f) Bar graph of NT diameters as a function of the carboxylate counterions sorted by increasing molecular weight (in parentheses). The star indicates the absence of NTs.

of different types of monovalent counterions. These counterions fall into two categories: (i) the small anions series (F^-, Cl^-, NO_3^-, Br^-, I^-, and ClO_4^-), which mostly gathers anions taken from the Hofmeister series and (ii) the carboxylate ions series (formate, acetate, L- and D-lactate, pivalate, benzoate, and phenyl acetate).

Transmission electron micrographs (see representative pictures in Figure 2a,b) show that NTs are formed with all the counterions studied but formate. From a structural point of view, the attenuated total reflection (ATR)-FTIR spectra (Figure 2c) exhibit all the features expected and previously described in the amide I vibration region (1600−1700 cm^{-1}):[20,21] the high- and low-frequency bands of an antiparallel β-sheet at 1694 and 1614 cm^{-1}, a turn at 1664 cm^{-1}, and a random conformation at 1640 cm^{-1}. These band positions are governed by the peptide backbone conformation and the hydrogen-bonding pattern; they are thus correlated with the molecular and supramolecular packing of the NTs.

SAXS data (Figure 2d) confirm these observations that the peaks at 0.35 $Å^{-1}$ come from the antiparallel β-sheet network and that all the patterns exhibit the typical oscillations of X-ray scattering of hollow cylinders.[25] The NT diameter can be extracted by fitting these oscillations with normalized zeroth-order Bessel functions (see Experimental Section).

Figure 2e shows that the ionic radii (see material and methods for calculation) of the small ions, i.e., fluoride (1), chloride (2), bromide (3), nitrate (4), iodide (5), and perchlorate (6), are proportional to the inverse of the NT diameters. However, there is no such obvious trend with the carboxylate series (Figure 2f). Although the pivalate molecule is supposedly bigger than the acetate, the NTs formed are thinner; and despite their similarity, L- and D-lactate lead to different sizes of tubes.

The plot of the ionic radii versus the inverse of the NTs diameters refers to the following relationship:

$$\delta_i = F - f - \left(2F\frac{e}{D_i}\right) \quad (3)$$

This relationship was determined from a geometrical model that takes into account the molecular and supramolecular structure adopted by the peptide within the inner layer of the NTs wall.[22] Interestingly, the y-intercept and the slope in this relationship are related to structural parameters that have been determined previously; e is the distance between the charges across the wall (that is the wall thickness of 18 Å); F and f_i are the lengths between two close contacts on the external and internal layers, respectively. In this model, F is constant, and $f_i = f - \delta_i$, f being a constant length, and δ_i a characteristic size related to the counterion. If the effect of the counterions on the NT diameter was only related to the size of the counterion, the slope $(F - f)$ and the y-intercept $(-2Fe)$ should give values in agreement with the structural parameters previously determined. Using F = 19.7 Å according the unit cell parameters,[21] the values of f and e extracted from the linear fit are 11 and 34.6 Å, to be respectively compared to 15 and 18 Å, according to SAXS data.[22] Therefore, although the trend supports the idea that the counterions participate in the inner layer of wall structure, the size criterion may not be enough to explain quantitatively the dependence of the NT diameter on the nature of the counterion, probably because the lever arm is weaker than with purely steric close contacts.

In a second series of experiments, we checked if the counterions can compete with another kind of ions present in solution as background salts. Since any change of counterion induces a modification of the NTs diameter, the samples were characterized by SAXS. Therefore, both lanreotide-acetate and lanreotide-chloride powders were solubilized at 10 % w/w in increasing amounts of sodium acetate or sodium chloride salts, i.e., lan-acetate in sodium acetate or sodium chloride and lan-chloride in sodium acetate or sodium chloride up to 175 mM. In Figure 3a, we plotted the evolution of the NT diameter obtained with the molar ratio Y/X, where X is the counterion bound to the peptide in the lyophilized salt and Y the competing anion used in the background salt.

When the ionic strength is increased up to 175 mM with the same anionic species as the initial counterion, i.e., lan-acetate in sodium acetate (A/A) or lan-chloride in sodium chloride (C/C), the NT diameter barely changes (±0.2 nm). Yet, the SAXS radial integration profiles display fewer oscillations with increasing ionic strength, and they do not go down to zero

dx.doi.org/10.1021/ja210299g | J. Am. Chem.Soc. 2012, 134, 723−733

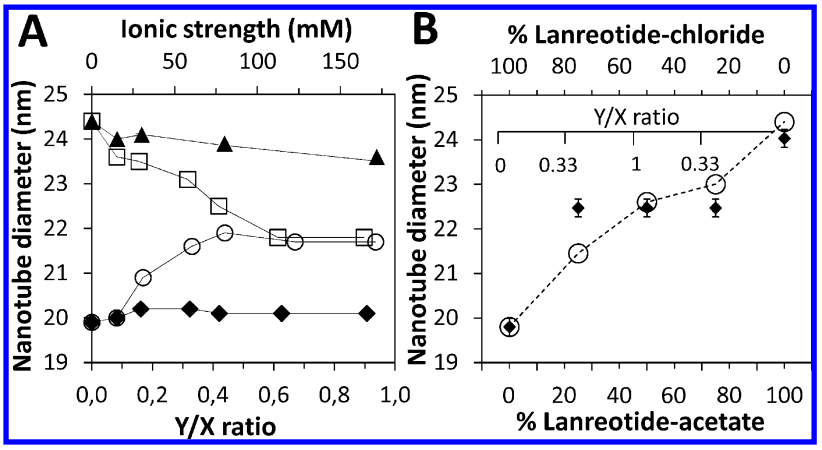

Figure 3. (a) Influence of the ionic strength on the NTs diameter and competition between acetate and chloride counterions. Y is the competitor used to set the ionic strength of the solvent, and X is the counterion bound to the lanreotide in the lyophilized salt. Each series is named Y/X. A = acetate and C = chloride: closed triangles, A/A; closed diamonds, C/C; open squares, C/A; and open circles, A/C. (b) Lan-acetate and lan-chloride mixtures. Open circles are experimental diameters measured by SAXS. Closed diamonds are fitted diameters obtained with the model devised in the discussion.

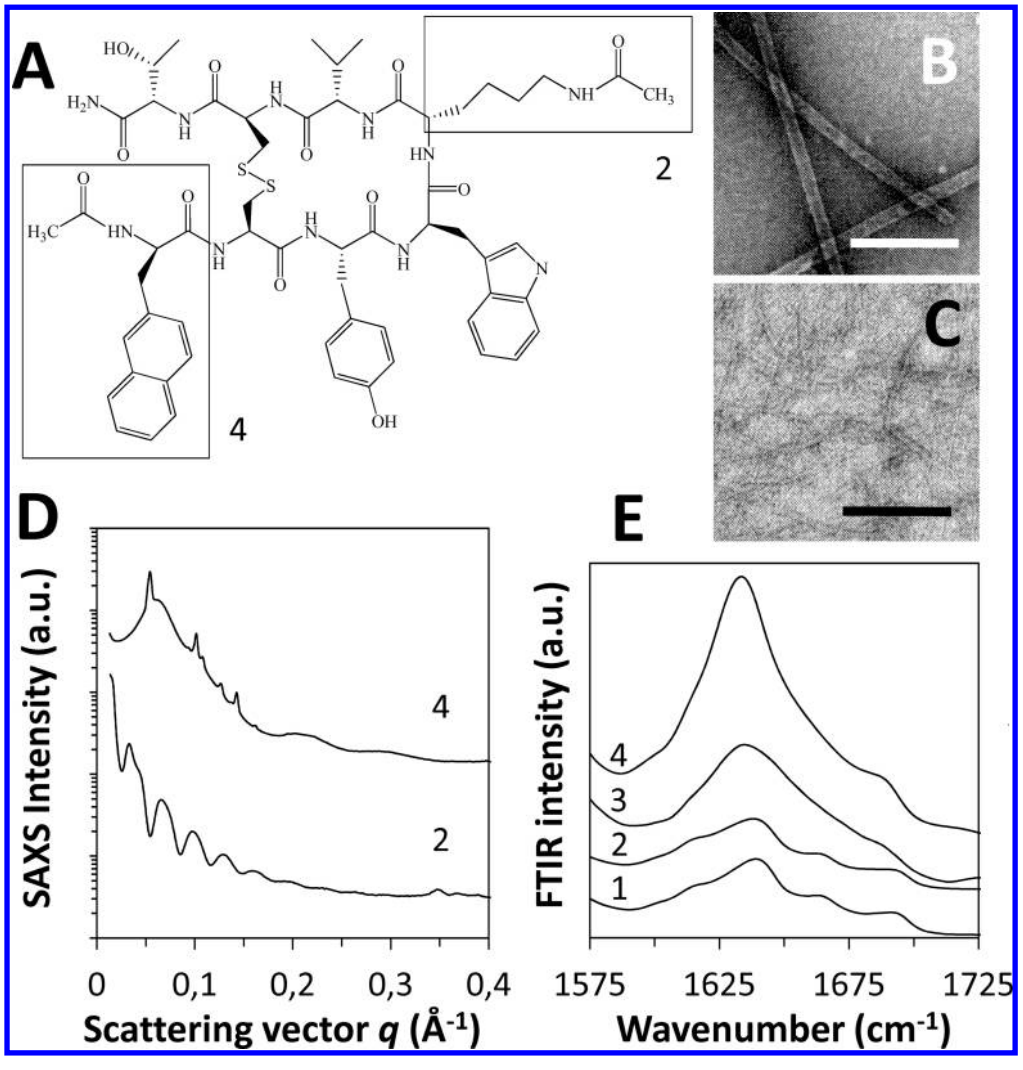

Figure 4. Lanreotide charge suppression by acetylation of the amine functions. (a) Lan-Ac-K-ac-Nter formula. In this derivative, the two positive charges of the lanreotide, located on the first and fifth positions are replaced by an acetyl function. (b) TEM micrograph of the negatively stained Lan-Ac-K peptide. Scale bar = 200 nm. (c) TEM micrograph of the negatively stained Lan-Ac-Nter peptide. Scale bar = 200 nm. (d) SAXS profiles of Lan-ac-Nter and of Lan-Ac-K peptides. (e) FTIR spectra of 10 % w/w lanreotide solutions and of the three derivatives: 1, lanreotide; 2, Lan-Ac-K; 3, Lan-Ac-K-Ac-Nter; and 4, Lan-Ac-Nter.

dx.doi.org/10.1021/ja210299g | J. Am. Chem.Soc. 2012, 134, 723–733

anymore, indicating a slight increase of the polydispersity (see Supporting Information). On the other hand, when the ionic strength is set with a different anionic species, i.e., lan-acetate in sodium chloride (C/A) and lan-chloride in sodium acetate (A/C), the measured NT diameter clearly changes. Furthermore, the diameter reaches in both conditions a plateau at 22.1 ± 0.9 nm, an average value between the lan-acetate and lan-chloride NT diameters. This plateau is already reached when the proportion of added counterions is only half of the initial ones. The diameter change indicates that counterions are only partially bound to lanreotide and can be spontaneously replaced by others. Moreover, the convergence plateau suggests that only half of the counterions are easily replaced and that there is no specific affinity of the peptide for one or the other counterion. However, this exchange could either occur randomly or only at specific sites.

In another set of experiments lan-acetate and lan-chloride powders were mixed in 1:3, 1:1, and 3:1 proportions. Compared to the previous experiment, the ionic strength of the solution in equilibrium with the NTs is set by the nonassembled peptide. Upon solubilization in pure water and for the three different mixtures, monodisperse NTs, whose diameter depends on the chloride/acetate ratio, form (Figure 3b).

The relative importance of the two positive charge sites of the lanreotide, the amine on the first position and the amine on the lysine side chain on the fifth position, respectively, has been assessed by acetylation of one (Lan-Ac-Nter), the other (Lan-Ac-K) or both (Lan-Ac-K-Ac-Nter). Indeed, the main consequence of this chemical modification is to neutralize the charges. The detailed sequence of the peptides is reported in Table S1, Supporting Information, and Figure 4a.

The acetylation of both amines (Lan-Ac-K-Ac-Nter) renders the peptide insoluble in water. Indeed, the absence of charges kills the electrostatic repulsions that stabilize the original peptide. The ATR-FTIR spectrum only reveals broad amide I and II bands (Figure 4b). On the contrary, the two other derivatives, on which only one of the two positive charges is suppressed, remain soluble, albeit poorly in the case of Lan-Ac-K. When the N-terminal charge is suppressed (Lan-Ac-Nter), thin filaments are observed by TEM above 25−30 % w/w (Figure 4c), and the ATR spectrum reveals a sharp peak at 1633.4 cm^{-1} (with a shoulder at 1683.6 cm^{-1}), indicating a parallel β-sheet organization (Figure 4e). The SAXS pattern shown in Figure 4d displays a few diffraction peaks.

On the other hand, the acetylation of the amine on the lysine side chain (Lan-Ac-K) leads to the formation of NTs whose features in TEM, ATR, and SAXS (Figure 4b,d,e, respectively) are similar to those observed with lanreotide (see refs 20 and 21 and the previous section). However, the diameter is only 19.7 nm, hence smaller than that of lanreotide NTs (24.4 ± 0.2 nm). Counterion exchanges have also been carried with Lan-Ac-K, but a comprehensive set of data was difficult to gather because of the low solubility of this peptide. Nevertheless, NTs diameter with chloride was measured to be 18.9 nm, a value close to the one obtained with acetate (i.e., 19.7 nm). The structural influence of the counterions positioned at the N-terminal thus seems to be small.

In this section, we have shown that counterion size modulates the NTs diameter and concluded that they participate in the wall structure. However, a geometrical model involving only the size of the counterion is not enough to explain this dependence. Moreover, the competition results suggest that the counterions sites are probably not equivalent, just as the two positive charges on the peptide (the amines of the N-ter and of the lysine) play different roles in the assembly process. Indeed, since the inner and outer layers of the NT walls are not symmetric, there are four different sites.

DISCUSSION

In our previous reports, the self-assembly mechanism and the molecular and supramolecular organization of lanreotide salt NTs have been characterized together with the corresponding phase diagram.[20,21,23] In these different studies, we have often been led to think that the electrostatic repulsions could play a crucial role in the control of the process without, however, directly addressing this question. Therefore, the present work is focused on the role of charges in the supramolecular organization.

The first section of the discussion will focus on the solutions below the CAC. Then the consequences of the NTs appearance on the solution will be discussed in terms of electrostatics. Finally, the structural role of the counterions and their localization in the NT wall will be treated.

Lanreotide in Solution: Monomers, Dimers, and Counterions (below the CAC). Below the critical concentration of 15−20 mM, the pH is buffered around 6.3 by the peptide amines (lysine side chain and N-terminal) and the acetate counterions, whereas the osmolarity of the solution increases with the peptide concentration. As expected when a monomer−dimer equilibrium takes place,[23] this increase is not linear. However, the fit of the experimental data (Figure 1c) shows that while the counterions of the monomers are completely dissociated, three out of four counterions are closely associated to the dimers. Instead of four charges, the dimers therefore exhibit a single one; the three others being neutralized by closely interacting counterions. The apparent charge of the dimer is lower than that of the monomer. As a consequence, the dimer−dimer interaction is less repulsive than monomer−monomer interaction. Interestingly, our previous work evidenced that the building block of the NTs is the dimer, and this analysis gives physicochemical arguments to back up this view.

Futhermore, the strong interaction between the peptide dimer and its counterions has a direct consequence not only on the osmotic pressure but also on the ionic strength of the liquid phase at the CAC. Indeed, for lanreotide-salt concentration higher than the CAC, NTs are formed and are in equilibrium with a solution of monomers and dimers of peptides that represent an electrolyte medium. The total osmotic pressure of this medium, calculated from the osmolarity ($\Pi = RT\rho_{water}\pi$, where ρ_{water} is the density of water and π the osmolarity of the peptide solution at the CAC), is 86 kPa. The ionic strength I, which strongly depends on the nature of the ions in solution, is calculated as follows:

$$I = \frac{1}{2}\sum_i c_i z_i^2 = \frac{1}{2}([M]*2^2 + [D] + [AcO^-]) \quad (4)$$

where the c_i is the concentration of each ion in solution and z_i their respective valences. In accordance with the osmometry measurements, the monomer M is considered as a dication, but the dimer D as single charge cation. Finally, the ionic strength is 36 mM instead of 80 mM for a fully dissociated system.

The NTs Liquid Phase Coexistence (above the CAC). In the coexistence domain, the number of NTs increases, while

dx.doi.org/10.1021/ja210299g | J. Am. Chem.Soc. 2012, 134, 723−733

the concentration of free monomers and dimers in equilibrium remains constant. However, because of the large diameter of the NTs and their similarly large interdistance, the two phases are not separated but interlocked. This section aims at giving a picture of these interacting species.

From an electrostatic point of view, the appearance of NTs in the solution can be seen as the creation of a positively charged surface that generates an electrostatic potential acting on the ionic species in presence. The solution can be characterized by a Debye length κ^{-1} beyond which the ionic species in solution screens the electric field created by such a surface.[26] This characteristic length is defined by

$$\kappa^{-1} = \sqrt{\frac{\varepsilon_r \varepsilon_0 k_B T}{2 N_A e^2 I}} \tag{5}$$

where ε_r and ε_0 are the dielectric constants of water and of the vacuum respectively, k_B the Boltzmann constant, T the temperature of the system, N_A the Avogadro number, e the elementary charge, and I the ionic strength of the solution as calculated in eq 4. At the CAC above this threshold, the concentration of free ions barely increases, and the Debye length is equal to 1.9 nm. Since this value is small compared to the diameter of the NTs (>20 nm), the peptide wall seen by an ion can be considered as a plane. Additionally, knowing the surface S = 377 Å^2 (reference[21]) of a unit cell containing two molecules (and hence four positive surface charges), we can estimate the maximum surface charge density of the bare NTs:

$$\sigma = -\frac{4*q}{S} = 0.17 \text{C}\cdot\text{m}^{-2} \tag{6}$$

However, we have previously seen that the 75% of the counterions were closely associated to the dimers, i.e., the NT building blocks, before their assembly in the NT wall. Taking into account this preliminary chemisorption, we expect that the surface charge density of the NT wall is only $\sigma_{chem} = 0.25*\sigma_{bare} = 0.0425$ C·m^{-2}.

A high charge density on a polyelectrolyte often triggers the condensation of counterions. This phenomenon has been well described by Manning's theory.[27] This theory states that the condensation occurs when the Coulombic potential energy (electrostatic interaction) overcomes the entropy (thermal motion). Thus, if the bare surface charge density σ_{bare} is lower than a critical surface charge density σ_{crit}, no condensation is observed, while above, condensation occurs to maintain the effective charge density equal σ_{crit}. In the case of a charged plane, the critical surface charge density[28] is defined by

$$\sigma_{crit} = -\frac{e\kappa*\ln(\kappa\lambda_B)}{2\pi n \lambda_B} = 0.019 \text{ C}\cdot\text{m}^{-2} \tag{7}$$

where e is the elementary charge, κ the inverse of the Debye length (see eq 4 supra), λ_B the Bjerrum length in water (~0.7 nm), and n is the valence of the counterions (here, −1). Compared to σ_{chem}, the obtained value of σ_{crit} indicates that ~55% of the remaining free counterions should condense on the bare surface. Thereby, only ~11% of the counterions, not counting those in the liquid phase in equilibrium with the monomers and dimers, remain free in the solution, a value close to the 10% measured on the osmolarity plot.

Let us now give a closer look at the effect of such a plane on the ionic species in the solution. This situation can be modeled by the classical theory of the electric double layer as stated by Gouy and Chapman[29−31] in which the solvent is assumed to be a continuous medium and the ionic species point charges. The concentration of any ion $i_{+/-}$ at any distance x from the NT wall is then given by a Boltzmann law such as

$$[i_{+/-}](x) = [i_{+/-}]_\infty * \exp\left(\frac{-zne\psi(x)}{k_B T}\right) \tag{8}$$

where z and n are the sign and valence of the ion, $\psi(x)$ the electric potential at x nm from the NT wall, k_B the Boltzmann constant, and T the temperature of the system. The subscripts ∞ denotes the concentrations in the bulk solution.

Figure 5a shows that as soon as NTs are formed, their vicinity is enriched in anions and depleted in cations.

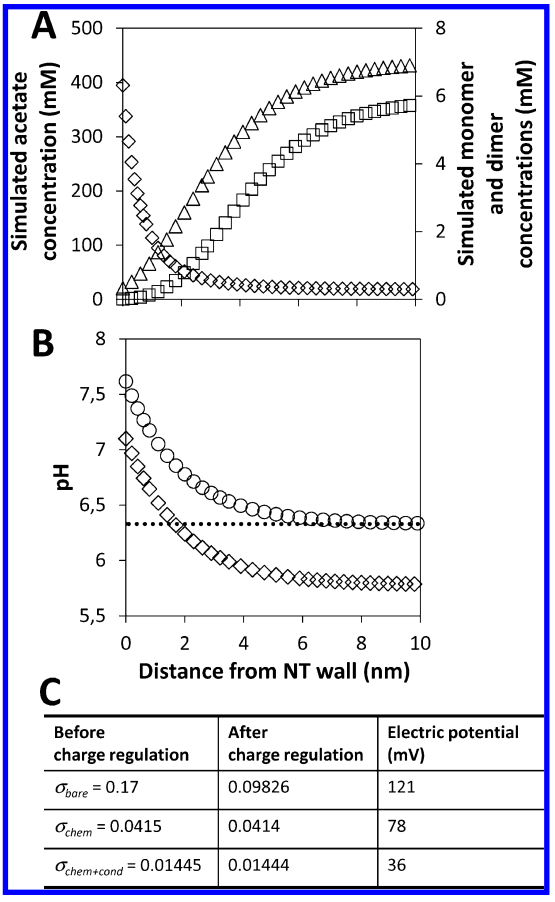

C

Before charge regulation	After charge regulation	Electric potential (mV)
σ_{bare} = 0.17	0.09826	121
σ_{chem} = 0.0415	0.0414	78
$\sigma_{chem+cond}$ = 0.01445	0.01444	36

Figure 5. Simulation of the electrostatic effects induced by the appearance of NTs in the solution calculated from the experimental pH and using an initial surface charge density σ_{chem} = 0.0415. (a) Simulated concentration profiles of the monomer (divalent cation, open squares), dimer (monovalent cation according to osmolarity fits, open triangles), and acetate (open diamonds) as a function of the distance from the NT wall at pH_∞ = 5.78. (b) Simulated pH profile of protons with (pH_∞ = 5.78, open diamonds) and without (pH_∞ = 6.33, dotted horizontal line) NTs in the solutions. An additional profile is plotted in the hypothetic case where the bulk solution would still be buffered at pH = 6.33 in the presence of NTs (open circles). (c) Table summarizing the effect of charge regulation for different initial surface charge densities.

Interestingly, because of their lowered charge number discussed previously, the dimers are allowed to come closer to the NT wall than the monomers, which again is consistent with their role as building blocks. Protons are as well repelled from the

dx.doi.org/10.1021/ja210299g | J. Am. Chem.Soc. 2012, 134, 723−733

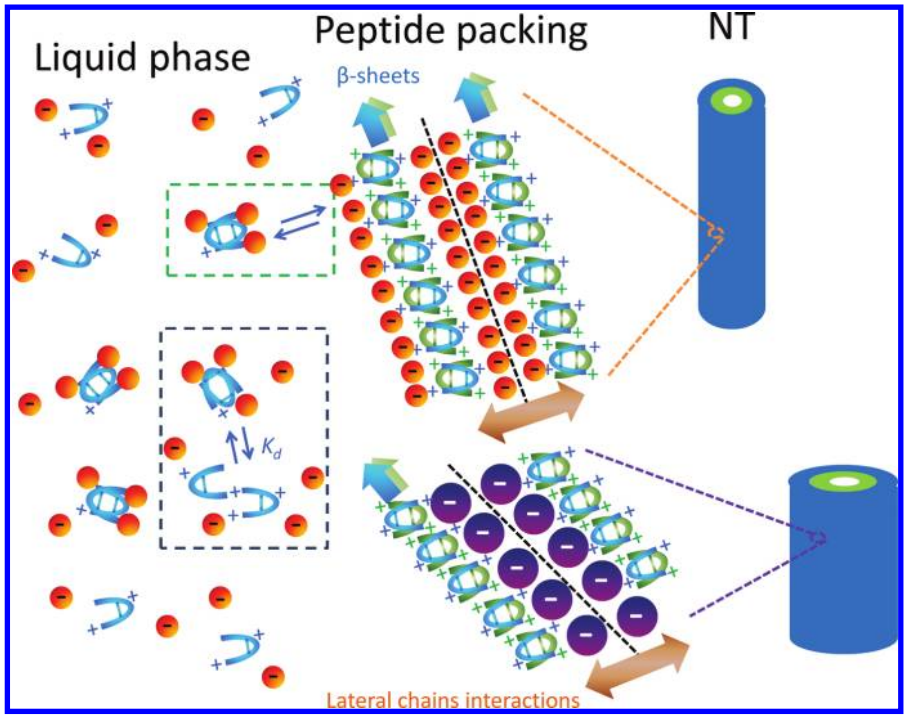

Figure 6. Cartoon summarizing the location of the counterions in the liquid hase and in the NTs walls. On the left: the liquid phase containing monomers, dimers, and counterions. Middle: Planar view of the peptide packing in the NT wall. The backbones of the lanreotide molecules are represented by the hairpins; for clarity, the hydrogen bonds that form the β-sheets are not represented. Green represents the inner layer of the wall and blue the outer layer. The dashed lines materialize the "close contact areas" between two β-sheets. Note that the counterions (not to scale) are modifiying the angle between the β-sheets and the lateral chains interactions. On the right: NTs of different diameters as a result of using spherical counterions of different sizes.

NTs vicinity, and Figure 5b illustrates the pH profile in the solution. While in the absence of NT, the pH is buffered around 6.33, and as soon as NTs are formed, their vicinity is depleted in protons ($pH_0 \approx 7$) leading, by consequence, to the enrichment of the bulk solution ($pH_\infty \approx 5.75$) (Figure 5b). In return, the important increase of the surface pH influences the protonation state of the amines. As a consequence, the wall surface charge density σ is not fixed and is subject to a phenomenon known as charge regulation.[32] The corresponding electric potential ψ_0 can be calculated by equalizing the Grahame equation (eq 9) and the expression of σ using the dissociation constant K_a of the amines of the peptidic wall (eq 10):

$$\sigma = \sqrt{8\varepsilon_r\varepsilon_0 k_B T} * \sqrt{I} * \sinh\left(\frac{e\psi_0}{2k_B T}\right) \quad (9)$$

$$\sigma = \frac{[H^+]_\infty * \exp\left[-\frac{e\psi_0}{kT}\right]}{K_a + [H^+]_\infty * \exp\left[-\frac{e\psi_0}{kT}\right]} \quad (10)$$

where ε_r and ε_0 are the dielectric constants of water and of the vacuum, respectively, and I the ionic strength of the solution. Thereby, for each pH_∞ value, we can calculate σ, ψ_0, and the concentrations $[i_{+/-}](x)$. Since there is a constant feedback between the pH in the bulk solution, the pH in the vicinity of the NTs, and the state of protonation of the amines of the NT walls, an iterative optimization is needed to calculate the exact surface charge density, using as a criterion the convergence of the apparent constant $K_{app} = [H^+]_\infty[\text{R-NH}_2]/[\text{R-NH}_3^+]_0$. We estimated the charge regulation for three different surface charge densities for bare NTs (σ_{bare} = 0.17 C·m^{-2}), before (σ_{chem} = 0.0425 C·m^{-2}), and after the counterions condensation ($\sigma_{chem+cond}$ = 0.0144 C·m^{-2}). If in the first case (see Figure 5c), the charge regulation is significant, while in the two others it is only marginal. However, the slight increase of pH_0 is always observed, supporting the idea that in the presence of NTs, the pH of the solution is buffered by the NT walls and not anymore by the free species in solution. Interestingly, the concentration profiles of every charged species reaches the onset of a plateau at a distance lower than the NT radius, meaning that part of the solution inside the NTs has the properties of the bulk solution.

Structural Role of the Counterions in the NT Wall. We have gathered several experimental evidence that the counterions are an integral part of the NT wall. Osmolarity measurements indeed show that in the NT existence domain, almost no increase of osmolarity is observed, indicating that the counterions strongly interact with the NTs in greater proportions than expected from Manning's condensation theory. Moreover, the dependence of the NT diameter with the size of the counterions suggests that they enter the NT wall structure.

Lanreotide NT walls are made of a curved 2D crystal formed by two nonequivalent peptidic layers represented in the sketch Figure 6. The wall thickness is the result of the face-to-face association of the monomers into dimers by segregation of the aromatic and aliphatic residues.[21] The inner and outer layers of the wall are stabilized by intermolecular hydrogen bonds perpendicular to the hairpins and interactions between lateral chains parallel to the hairpins. Close contact sites, for example, between tryptophan residues of adjacent peptides, are located in between two β-sheets (black dashed line). These close contacts have been previously shown to offer an efficient lever

dx.doi.org/10.1021/ja210299g | J. Am. Chem.Soc. 2012, 134, 723−733

arm to control the NT diameter.[22] Indeed, the proposed geometric model highlighted the fact that in order to increase the NT diameter, it was necessary to increase the steric hindrance of a residue involved in a close contact inside the inner layer. This region also shelters the peptide charges. Since 90% of the counterions are adsorbed or condensed on the NT wall and their size modulates the NT diameter, as the present results suggest, it is very likely that they are also located in this same region. If we consider a dimer inside the NT wall, four different counterion sites can be counted: two in the inner layer and two in the outer layer. In each layer, one counterion is associated to the terminal amine and the other on the lysine side-chain amine.

The fact that the NT diameter is roughly proportional to the counterion ionic radius suggests that the structural role of the counterions is mostly steric and that their effect is most important in the inner layer, by analogy with the results obtained with nonionic close contacts.[22] Additional evidence pleading for this "electrostatic close contact" explanation comes from the experiments carried with the Lan-Ac-K peptide. In the NT walls formed by this peptide, all the charges are staggered in both layers, hence preventing the possibility of direct face-to-face interaction between counterions; indeed our experiment shows that the Lan-Ac-K NT diameter is much less sensitive to ion exchange than lanreotide.

The absence of correlation with the carboxylate series could find several possible explanations: (i) these counterions are so large that the opposite internal and external effects more or less cancel out; (ii) the effectiveness of the "lever arm" of more complex counterions might depend on their conformation; (iii) part of these molecules might be outside the wall, hence having no real influence on the parameter cell whatever their size; and (iv) finally, other ionic properties, such as polarizability, free energy or entropy of hydration, could be involved.

Modeling the Specific Role of Each Counterion Site. The experiments carried out with competing kinds of anions show that the different charged sites in NTs walls are not equivalent (Figure 4a). Indeed, the diameter is not strictly proportional to the ratio of Y/X counterions.

In order to estimate the specificity of the different sites, we devised a simple global model whose main assumption is that all the effects are additive. The NT diameter D can thus be written as

$$D = D_0 + \Sigma\alpha_i R_j \qquad (11)$$

where R_j represents the steric hindrance due to the counterion and/or any chemical modification of the residue (e.g., acetylation) in any site and the α_i the specific weight assigned to each site. Finally, D_0 is an arbitrary constant. Using this formalism, a set of data can be described by a system of equations to solve (see Table 1 below and details in Supporting Information).

The set was limited to the lan-acetate and lan-chloride mixtures (data of Figure 3b) and the acetate and chloride salts of Lan-Ac-K. The best, but not perfect, fit obtained with this model is represented in Figure 3b. It leads to the conclusion that both α_{ext} are equal to zero, i.e., that the external sites are not involved in the control of the NT diameter (at least for what chloride and acetate counterions are concerned). On the contrary, the sites located in the inner layer directly dictate the diameter. This prevailing role of the inner sites can be intuitively explained by the fact that the curvature of the wall compels the molecules in the inner layer to be slightly more densely packed. As a consequence, the charged sites and the close contacts are more sensitive to any steric modification, such as counterion exchange (present paper) or chemical mutations, in the inner layer.[22] Also, even though the values of the parameters could not be linked to physical ionic parameters, the model indicates that α_{inner} lysine is twice higher than α_{inner} N-ter, which implies that the inner lysine site is a stronger lever arm. This is also consistent with the fact that changing the counterions only in the inner N-ter site (on the Lan-Ac-K peptide) barely modifies the NT diameter. However, the N-terminal charge must play a crucial role in terms of assembly control since its deletion prevents the NT formation. At the same time, the lysine charge imparts a much higher solubility to the peptide than the N-terminal one.

Table 1. Set of Equations Needed to Model the Role of Each Ionic Site (upper part) and Parameter Values of the Best Fit (lower part)

experiment	D_{exp} (nm)	D_{theo} (nm)	% deviation
lan-acetate	24.4	24.0	1.6
lan-chloride	19.8	19.8	0
lan-Ac-K-acetate	19.7	20.1	2
lan-Ac-K-chloride	18.9	18.5	2.2
lan-acetate/lan-chloride 50:50	22.6	22.5	0.4
lan-acetate/lan-chloride 25:75	21.45	22.5	4.9
lan-acetate/lan-chloride 75:25	23	22.5	2.2

α_{ext_K}	α_{ext_Nter}	α_{in_K}	α_{in_Nter}	$R_{acetate}$	$R_{chloride}$	$R_{N\text{-}acetyl}$
0	0	1	0.5795	4.95	2.28	1

However, as mentioned above, this model does not perfectly fit the experimental data. Indeed, for 25−75% and 75−25% acetate-chloride mixtures the experimental values are respectively below and above the theoretical ones (Figure 3b). This suggests that although there is a clear affinity for the inner sites, there is still a partition that is not taken into account by our model. By comparing the theoretical and experimental diameter values, we can estimate that two-thirds of the counterions partitioned on the inner sites for one-third on the outer sites.

In this section, we have described the structural role of the counterions in terms of steric effects and specific sites, supported by a good correlation between the counterions radii and the NT diameters for the mineral anions.

CONCLUSION

We have shown that the state of dissociation of the counterions depends on the level of assembly of the lanreotide peptide. Indeed, if the counterions are completely dissociated from the monomers, 75% of them are chemically adsorbed on the dimers. When the NTs are formed, an additional 15% of them condense on their surface. Ultimately, the NTs surface charge density is much less than that of bare NTs. Moreover, we have also demonstrated that counterions are not simply regulating the charges on the surface of the NTs but are also playing an important structural role, since they can tune the diameter of the NTs in a 19−26 nm range. This observed counterion effect is thus anion specific. Although such a specific ionic effect never relies on a single parameter but is the result of a complex balance, we could identify the counterion size as the main parameter under certain conditions. This steric effect is further supported by the localization of the peptide charged sites in areas involved in structural close contacts.

We have also evidenced that the counterion adsorption sites where the counterions condense are also specific. Thanks to a

dx.doi.org/10.1021/ja210299g | J. Am. Chem.Soc. 2012, 134, 723−733

simple model we could distinguish the weight of the different charged sites on the peptide. More generally, the two amines clearly play different roles in terms of peptide solubility, self-assembly morphology control, and diameter modulation.

Overall, this study deepens our understanding of the structure of the self-assembling lanreotide system and opens the way to using charges and counterions as additional structural parameters. Beyond mere size control, functionalization through counterions can also be envisioned.

EXPERIMENTAL SECTION

Materials. Lanreotide was obtained from Ipsen Pharma (Barcelona, Spain) and the derivatives were synthetized by solid-phase fluorenylmethyloxycarbonyl (FMOC) chemistry as described in ref 22. Peptide sequences are lanreotide: H-D-2-Nal^1-*cyclo*(Cys^2-Tyr^3-D-Trp^4-Lys^5-Val^6-Cys^7)-Thr^8-NH$_2$; Lan-Ac-Nter: Ac-D-2-Nal^1-*cyclo*(Cys^2-Tyr^3-D-Trp^4-Lys^5-Val^6-Cys^7)-Thr^8-NH$_2$; Lan-Ac-K-Ac-Nter: Ac-D-2-Nal^1-*cyclo*(Cys^2-Tyr^3-D-Trp^4-Lys(Ac)^5-Val^6-Cys^7)-Thr^8-NH$_2$, and Lan-Ac-K: H-D-2-Nal^1-*cyclo*(Cys^2-Tyr^3-D-Trp^4-Lys(Ac)^5-Val^6-Cys^7)-Thr^8-NH$_2$.

NMR Analysis. The synthesized peptides were controlled by 1H-NMR on a Bruker Avance 400 Ultrashield. Spectra were recorded at room temperature at 400 MHz, and samples were dissolved in D_2O at a concentration of approximately 5 mM. The D_2O singlet signal was set up at 4.79 ppm. Chemical shifts are given in ppm and the coupling constants in Hz (see Supporting Information text for details on the peptide characterization).

Sample Preparation and Counterions Exchange by Deprotonation/Reprotonation Procedure. All peptides were obtained as an acetate salt powder, and acetate counterions were exchanged following the procedure exposed in ref 33 with slight modifications; the powder, insoluble at basic pH, was washed for 15 min at 4 °C with a 58 mM NaOH solution. The volume was calculated ad hoc so that the hydroxide ions neutralize all the peptide charges with only 10% excess. After several rinses with deionized water followed by centrifugation at 4 °C for 5 min at 2500 g and removal of the supernatants, the pellet/hydrated powder was freeze dried. The dry powder containing the neutral form of the peptide could then be solubilized in an acidic solution containing enough charges of the desired counterion to reprotonate the peptide. After addition of deionized water to dilute the peptide solution below 1 % w/w, the solution was once more freeze-dried. The obtained powder could then be dissolved in deionized water to the desired concentration.

For this study we exchanged the acetate counterions for fluoride, chloride, nitrate, bromide, iodide, perchlorate, formate, pivalate, L- and D-lactate, benzoate, phenylacetate, and camphorsulfonate by using the corresponding acids. The acids were obtained from Sigma-Aldrich with at least 99% purity. HF was manipulated with the usual safety measures under an appropriate fume hood.

Osmometry and pH-metry. Osmotic pressure of the solutions was measured by freezing point depression method with a Roebling automatic micro-osmometer. The pH was measured with a pH-meter (Hanna instruments) equipped with a microprobe in a thermostated room. The solutions were degassed with argon beforehand.

TEM. The morphology of the supramolecular structures formed by the peptides was assessed with a Philips CM12 electron microscope operated at 80 kV. A drop of the solution at 3−5 % w/w was put on a copper grid covered with a carbon film (Agar Scientific). After blotting off of the excess liquid, the material was stained with 2% uranyle acetate or 2% ammonium molybdate.

SAXS. SAXS experiments were either performed at the SWING beamline at the SOLEIL synchrotron facility (Gif-sur-Yvette, France) or with a rotating anode laboratory setup. X-ray patterns were detected and recorded via a chip charge-coupled device (CCD) camera detector. The samples were inserted in 1.3−1.6 mm round glass capillaries and centrifuged at the bottom. The scattering intensities as a function of the radial wave vector, $q = 4\pi/\lambda \times \sin\theta$, were determined by circular integration (Fit2D, ESRF, Grenoble, France), and tubes diameter were, when present, estimated by fitting the corresponding oscillations by normalized zeroth-order Bessel functions, $J_0^2(q\cdot r_0)/q^2$, (see ref 25).

FTIR Spectroscopy. ATR-FTIR spectra were recorded at a 4 cm^{-1} resolution with a Bruker IFS 66 spectrophotometer equipped with a 45° N ZnSe ATR attachment. The spectra obtained resulted from the average of 30 scans and were corrected for the linear dependence on the wavelength of the absorption measured by ATR. The water signal was removed by subtraction of pure water spectrum. Analysis of the conformations of the peptides was performed by deconvolution of the absorption spectra as a sum of Gaussian components with PeakFit 4.12 (Seasolve Software Inc.).

Calculation of the Counterion Ionic Radii and Computational Details. In order to estimate the size of the counterions, we calculated their solvent excluding surface. The ionic radii used to plot Figure 2e are derived from the sphere that would define the same surface. Calculations were carried out at the DFT level using the Gaussian 03[34] package by means of the hybrid density functional B3PW91.[35,36] For all atoms, except hydrogen, the Stuttgart−Dresden pseudopotentials were used in combination with their associated basis sets.[37] For hydrogen, the all-electron 6-31G basis set was used. Each molecular anion was optimized without any geometry restriction. Optimizations have been carried out in water using the CPCM implicit solvatation model.[39] The cavity of the solute has been defined using Pauling−Merz−Kollman radii. The nature of the stationary point optimized has been verified by means of an analytical frequency calculation. The volume of the anion solvation shell in water has been estimated as the solvent excluding surface of the fully optimized solute.

ASSOCIATED CONTENT

Supporting Information

Complete refs 22 and 34. SAXS patterns of the data used in Figure 3. NMR analysis of the synthesized peptides. Cartesian coordinates and energy of the optimized anions. Details of the optimization for the global model fitting the specific counterions sites. This material is available free of charge via the Internet at http://pubs.acs.org.

AUTHOR INFORMATION

Corresponding Author

frederic.gobeaux@gmail.com; maite.paternostre@cea.fr

Present Address

¶Biomolecular Interaction Center, School of Biological Sciences, University of Canterbury, Christchurch, New Zealand.

ACKNOWLEDGMENTS

This work was supported by the biotechnology program of the French Agency for Research (ANR) with the SmartPep project. F.G. and N.F. were funded by Commissariat à l'Energie Atomique et aux Energies Alternatives. C.T. was funded by the Région Bretagne through a Ph.D. fellowship. The authors thank Luc Belloni and Thomas Zemb for clarifying discussions on electrostatics issues. Synchrotron SOLEIL (France) is acknowledged for beam time allocation. The TEM team platform (iBiTec-S/SB^{2}SM) is also acknowledged.

REFERENCES

(1) Collins, K. D. *Methods* **2004**, *34*, 300.
(2) Bloomfield, V. A. *Biopolymers* **1991**, *31*, 1471.
(3) Petrache, H. I.; Zemb, T.; Belloni, L.; Parsegian, V. A. *Proc. Natl. Acad. Sci. U.S.A.* **2006**, *103*, 7982.
(4) Wong, G. C. L.; Pollack, L. *Annu. Rev. Phys. Chem.* **2010**, *61*, 171.
(5) Hofmeister, F. *Arch. Exp. Pathol. Pharmacol.* **1888**, *24*, 247.
(6) Collins, K. D.; Washabaugh, M. W. *Q. Rev. Biophys.* **1985**, *18*, 323.

(7) Brady, J. E.; Evans, D. F.; Warr, G. G.; Grieser, F.; Ninham, B. W. *J. Phys. Chem.* **1986**, *90*, 1853.
(8) Gaillon, L.; Lelievre, J.; Gaboriaud, R. *J. Colloid Interface Sci.* **1999**, *213*, 287.
(9) Jiang, N.; Li, P. X.; Wang, Y. L.; Wang, J. B.; Yan, H. K.; Thomas, R. K. *J. Phys. Chem. B* **2004**, *108*, 15385.
(10) Jiang, N.; Li, P. X.; Wang, Y. L.; Wang, J. B.; Yan, H. K.; Thomas, R. K. *J. Colloid Interface Sci.* **2005**, *286*, 755.
(11) Maurer, E.; Belloni, L.; Zemb, T.; Carriere, D. *Langmuir* **2007**, *23*, 6554.
(12) Oda, R.; Huc, I.; Schmutz, M.; Candau, S. J.; MacKintosh, F. C. *Nature* **1999**, *399*, 566.
(13) Manet, K. Y.; Bassani, S.; Kiagus-Ahmad, D.; Oda, R. *Langmuir* **2010**.
(14) Oda, R.; Artzner, F.; Laguerre, M.; Huc, I. *J. Am. Chem. Soc.* **2008**, *130*, 14705.
(15) Brizard, A.; Dolain, C.; Huc, I.; Oda, R. *Langmuir* **2006**, *22*, 3591.
(16) Wang, Y. J.; Desbat, B.; Manet, S.; Aime, C.; Labrot, T.; Oda, R. *J. Colloid Interface Sci.* **2005**, *283*, 555.
(17) Stendahl, J. C.; Rao, M. S.; Guler, M. O.; Stupp, S. I. *Adv. Funct. Mater.* **2006**, *16*, 499.
(18) Grohn, F. *Macromol. Chem. Phys.* **2008**, *209*, 2295.
(19) Grohn, F.; Klein, K.; Brand, S. *Chem.—Eur. J.* **2008**, *14*, 6866.
(20) Valery, C.; Artzner, F.; Robert, B.; Gulick, T.; Keller, G.; Grabielle-Madelmont, C.; Torres, M. L.; Cherif-Cheik, R.; Paternostre, M. *Biophys. J.* **2004**, *86*, 2484.
(21) Valery, C.; Paternostre, M.; Robert, B.; Gulik-Krzywicki, T.; Narayanan, T.; Dedieu, J. C.; Keller, G.; Torres, M. L.; Cherif-Cheikh, R.; Calvo, P.; Artzner, F. *Proc. Natl. Acad. Sci. U.S.A.* **2003**, *100*, 10258.
(22) Tarabout, C.; et al. *Proc. Natl. Acad. Sci. U.S.A.* **2011**, *108*, 7679.
(23) Pouget, E.; Fay, N.; Dujardin, E.; Jamin, N.; Berthault, P.; Perrin, L.; Pandit, A.; Rose, T.; Valery, C.; Thomas, D.; Paternostre, M.; Artzner, F. *J. Am. Chem. Soc.* **2010**, *132*, 4230.
(24) Cui, H. G.; Pashuck, E. T.; Velichko, Y. S.; Weigand, S. J.; Cheetham, A. G.; Newcomb, C. J.; Stupp, S. I.; *Science*, *327*, 555.
(25) Oster, G.; Riley, D. P. *Acta Crystallogr.* **1952**, *5*, 272.
(26) Israelachvili, J. *Intermolecular and Surface Forces*; Academic Press, Inc.: Waltham, MA, 2010.
(27) Manning, G. S. *J. Chem. Phys.* **1969**, *51*, 924.
(28) Manning, G. S. *J. Phys. Chem. B* **2007**, *111*, 8554.
(29) Gouy, G. *J. Phys. (Paris)* **1910**, *9*, 31.
(30) Chapman. *Philos. Mag.* **1913**, *25*, 475.
(31) Moreira, A. G.; Netz, R. R. *Eur. Phys. J. E: Soft Matter Biol. Phys.* **2002**, *8*, 33.
(32) Ninham, B. W.; Parsegian, V. A. *J. Theor. Biol.* **1971**, *31*, 405.
(33) Roux, S.; Zekri, E.; Rousseau, B.; Paternostre, M.; Cintrat, J. C.; Fay, N. *J. Pept. Sci.* **2008**, *14*, 354.
(34) Frisch, M. J.;et al. Gaussian, Inc.: Wallingford CT, 2009.
(35) Perdew, J. P.; Chevary, J. A.; Vosko, S. H.; Jackson, K. A.; Pederson, M. R.; Singh, D. J.; Fiolhais, C. *Phys. Rev. B* **1992**, *46*, 6671.
(36) Becke, A. D. *J. Chem. Phys.* **1993**, *98*, 5648.
(37) Bergner, A.; Dolg, M.; Kuchle, W.; Stoll, H.; Preuss, H. *Mol. Phys.* **1993**, *80*, 1431.
(38) Ditchfield, R.; Hehre, W. J.; Pople, J. A. *J. Chem. Phys.* **1971**, *54*, 724.
(39) Tomasi, J.; Mennucci, B.; Cammi, R. *Chem. Rev.* **2005**, *105*, 2999.

■ NOTE ADDED AFTER ASAP PUBLICATION

This article was published ASAP on December 22, 2011. Due to a production error, this paper was published before all corrections were applied. The corrected version was posted on December 27, 2011.